Inorganic Chemistry

Article

pubs.acs.org/IC

DNA Photocleavage by Non-innocent Ligand-Based Ru(II) Complexes

Yangyang Zhang,[†,‡] Qianxiong Zhou,[*,†] Yue Zheng,[†,‡] Ke Li,[†,‡] Guoyu Jiang,[†] Yuanjun Hou,[†] Baowen Zhang,[†] and Xuesong Wang[*,†]

[†]Key Laboratory of Photochemical Conversion and Optoelectronic Materials, Technical Institute of Physics and Chemistry, Chinese Academy of Sciences, Beijing 100190, P.R. China

[‡]Graduate School of the Chinese Academy of Sciences, Beijing 100049, P.R. China

Supporting Information

ABSTRACT: In this work, we demonstrate for the first time that $[Ru(bpy)_2(R\text{-}OQN)]^+$ complexes (bpy = 2,2′-bipyridine, R-OQN = 5-chloro-8-oxyquinolate or 5-bromo-8-oxyquinolate) are able to generate hydroxyl radicals and cleave DNA effectively upon visible light irradiation. The potent electron-donating ability of the R-OQN-based non-innocent ligands gives the complexes a high reducing capability, favoring the generation of superoxide anion radicals from which hydroxyl radicals may be generated. More interestingly, halogen substitution plays an important role. When the 5-Cl- or 5-Br-8-oxyquinolate ligand is replaced by 8-oxyquinolate or 5-CH_3-8-oxyquinolate, the corresponding complexes lose their hydroxyl radical-generation and DNA photocleavage abilities. These findings open new applications for the non-innocent ligand-based Ru(II) complexes in the fields of biology and medicine, such as in photodynamic therapy (PDT).

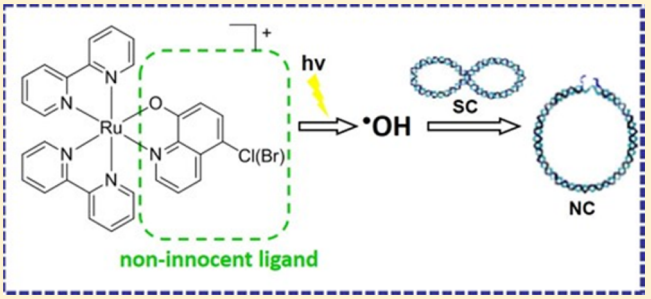

1. INTRODUCTION

By virtue of spatiotemporal selectivity in manipulating DNA functions, DNA photocleavers can confine cell death within diseased tissues, showing promising applications in photodynamic therapy (PDT), a noninvasive treatment modality for malignant tumors.[1,2] In this context, Ru(II) complex-based DNA photocleavers have been extensively studied because of their rich and tunable photophysical, photochemical, and redox properties.[3] They can photocleave DNA via a singlet oxygen ($^1O_2$), which is generated by energy transfer from the lowest-lying triplet excited state (the ^{3}MLCT state in general, but the ligand-centered $^3\pi\pi^*$ state in some cases) to O_2.[4] Alternatively, some Ru(II) complexes based on electron-deficient ligands such as tap, hat, and bpz (tap = 1,4,5,8-tetraazaphenanthrene, bpz = 2,2′-bipyrazine, and hat = 1,4,5,8,9,12-hexaazatriphenylene) can photodamage DNA via direct electron abstraction from DNA bases to their highly oxidizing ^{3}MLCT states.[5] Similarly, many Ru(II) complexes have been developed to cleave DNA via strongly oxidizing Ru(III) species generated upon photoinduced inter/intramolecular electron transfer from their ^{3}MLCT states to an electron acceptor.[6−8] Herein, we demonstrate for the first time that the non-innocent ligand-based Ru(II) complexes may photocleave DNA in a process totally different from those of the above-mentioned examples.

Non-innocent ligands earn their title from the fact that they participate in extensive π-overlap with metal-based atomic orbitals, resulting in highly delocalized molecular orbitals.[9a] Metal complexes with a non-innocent ligand exist either as a metal−ligand radical $M^{n+}(L^{\bullet})$ or as a higher valent metal complex $M^{(n+1)+}(L^-)$. Subtle changes in the electronic structure could significantly alter the redox site within the complex.[9b] Anionic redox active ligands bearing O^-, S^-, or NH^- donors usually display non-innocent properties due to their electron-donating character.[10] Ru(II) complexes based on such fascinating ligands have been intensively explored,[10e,11] and the electron-donating feature of the non-innocent ligands has been fully utilized to stabilize the high valent Ru center in water oxidation catalysis[12] and to promote electron injection from the Ru(II) center to TiO_2 in dye-sensitized solar cells.[13] 8-Oxyquinolate (OQN) derivatives are a class of non-innocent ligands, and their Ru(II) complexes were scrutinized with an emphasis on the photophysical, electrochemical, and electron-spin properties.[9a,14] Although OQN derivatives possess diverse biological activities and have been applied as pesticides and antifungal, antibiotic, and anticancer agents, the biological and medical applications of their Ru(II) complexes are still in their infancy.[15] Particularly, to the best of our knowledge, the DNA photocleavage activities of these complexes have not yet been examined. A possible reason may be that the OQN-based Ru(II) complexes generally show short excited-state lifetimes[14d] that are unfavorable for $^1O_2$ generation. Additionally, the strong electron-donating potency of the OQN-type ligands makes the resultant Ru(II) complexes difficult to utilize as electron acceptors in their excited state.[14d] The low oxidizing ability of the corresponding Ru(III) states of these complexes is also

Received: January 6, 2016

DOI: 10.1021/acs.inorgchem.6b00028
Inorg. Chem. XXXX, XXX, XXX−XXX

expected. All of these anticipations exclude their DNA photocleavage activity by way of the above-mentioned three mechanisms. We surmise the highly reducing property of the non-innocent ligand-based Ru(II) complexes may aid in the generation of superoxide anion radicals ($O_2^{-\bullet}$) from which hydroxyl radicals ($^\bullet$OH) may be formed via the dismutation reaction followed by the Harber–Weiss reaction (eq 3 in Scheme 1).[16] Following this idea, we examined the DNA

Scheme 1. Possible Mechanism for $^\bullet$OH Generation

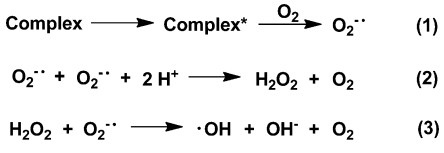

photocleavage activities of four Ru(II) complexes based on OQN-type ligands ($[Ru(bpy)_2(R\text{-}OQN)]^+$ (bpy = 2,2′-bipyridine; R-OQN = 5-substituted OQN; and R = H (**1**), Cl (**2**), Br (**3**), and CH_3 (**4**), Chart 1)) and demonstrate for the

Chart 1. Structures of the $[Ru(bpy)_2(R\text{-}OQN)]^+$ Complexes

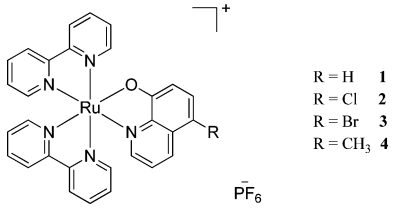

first time that some of them (**2** and **3**) can lead to $^\bullet$OH-mediated DNA cleavage efficiently, opening avenues for the use of the non-innocent ligand-based Ru(II) complexes as a new type of DNA photocleaver as well as a PDT agent.

2. RESULTS AND DISCUSSION

Photophysical and Electrochemical Properties. The hexafluorophosphate salts of the four complexes were prepared following literature procedures[9a,14a] and characterized by ^{1}H NMR and ESI-MS (Supporting Information). In good agreement with the reported results,[9a] **1**–**4** show MLCT absorption maxima in the range 502–508 nm (Table 1 and Figure S1), about a 50 nm red shift with respect to $[Ru(bpy)_3]^{2+}$. Additionally, the first oxidation and reduction potentials of **1**–**4** have a cathodic shift versus that of $[Ru(bpy)_3]^{2+}$ (Table 1 and Figure S2). For example, the

Table 1. Absorption, Electrochemical, and DNA Binding Properties of the Examined Complexes

complex	MLCT Abs_{max}[a] (nm)	$E_{1/2(ox)}$[b] (V) (vs SCE)	$E_{1/2(red)}$[c] (V) (vs SCE)	K_{app}[d] ($\times 10^6$ M^{-1})
$[Ru(bpy)_3]^{2+}$	450	1.28	−1.35, −1.54	
1	505	0.50	−1.52, −1.77	1.98
2	502	0.56	−1.51, −1.75	1.74
3	502	0.56	−1.51, −1.74	1.89
4	508	0.45	−1.53, −1.78	1.72

[a]MLCT absorption maxima in CH_3CN. [b]Oxidation half-wave potentials in CH_3CN. [c]Reduction half-wave potentials in CH_3CN. [d]Apparent binding constants toward CT-DNA obtained by EB displacement assay.

Ru^{3+}/Ru^{2+}-based redox potential of **1** appeared at 0.50 V (vs SCE), while that of $[Ru(bpy)_3]^{2+}$ appeared at 1.28 V. Similarly, the bpy-based reduction potential of **1** occurred at −1.52 V, while that of $[Ru(bpy)_3]^{2+}$ appeared at −1.35 V. Obviously, the cathodic shift of the Ru^{3+}/Ru^{2+} redox potentials, caused by the presence of an OQN ligand, is more significant than that of the bpy-based reduction potentials. Such a large shift is a result of the hybrid metal(dπ)-OQN ligand(π) molecular orbitals[9a,14a,17] leading to a MLLCT transition (from Ru(dπ)-OQN(π) to π^*(bpy)) with a narrowed energy gap, in good agreement with the absorption red shift of **1**–**4** with respect to $[Ru(bpy)_3]^{2+}$. From the point of view of electrochemistry, the large cathodic shift may be regarded as the stabilization of the Ru(III) state by the mixing of Ru(dπ)-OQN(π). While the cathodic shifts in redox potentials relative to $[Ru(bpy)_3]^{2+}$ are attributed to the π-donating influence of the R-OQN ligands, one cannot rule out an additional Coulombic contribution due to the reduced charge of **1**–**4**.[17] Notably, because of the non-innocent character of the R-OQN ligands, the Ru^{3+}/Ru^{2+} redox processes of **1**–**4** should involve the contribution of R-OQN^+/R-OQN; i.e., the oxidized complex exists in the form of a combination of $[Ru(III)(bpy)_2(R\text{-}OQN)]^{2+}$ and $[Ru(II)(bpy)_2(R\text{-}OQN^+)]^{2+}$.[9a,14a]

DNA Photocleavage and Binding Ability. We first examined the photocleavage abilities of **1**–**4** toward supercoiled (SC) pBR322 plasmid DNA using gel electrophoresis. As shown in Figure 1a, **2** and **3** cleaved DNA efficiently upon

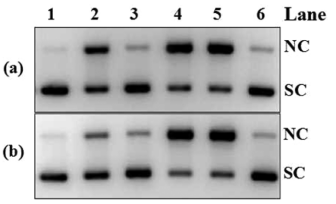

Figure 1. Agarose gel electrophoresis pattern of supercoiled pBR322 DNA (31 μM base pair) in an air-saturated Tris-CH_3COOH/EDTA buffer (pH 8.0, 8% DMSO) upon irradiation for 30 min in the presence of the examined complexes with >400 nm light at 50 μM (a) and with >470 nm light at 80 μM (b). Lane 1, DNA alone; lane 2, DNA + $[Ru(bpy)_3]^{2+}$; lane 3, DNA + **1**; lane 4, DNA + **2**; lane 5, DNA + **3**; lane 6, DNA + **4**. SC and NC denote supercoiled circular and nicked-circular forms, respectively.

irradiation at >400 nm as evidenced by the remarkable transformation of pBR322 DNA from the SC form to the nicked-circular (NC) form (lanes 4 and 5). In contrast, negligible DNA cleavage was observed for **1** and **4** under the same conditions (lanes 3 and 6). It is worth noting that halogen substitution is crucial for DNA photocleavage, and **2** and **3** can photocleave DNA more efficiently than $[Ru(bpy)_3]^{2+}$. Similar results were also observed when samples were irradiated with light at >470 nm (Figure 1b).

Control experiments were conducted to explore the DNA cleavage mechanism. Without irradiation, both **2** and **3** lost their DNA cleavage abilities (Figure S3). Additionally, irradiation under a N_2 atmosphere also eliminated their DNA cleavage abilities (lane 7 in Figure 2 for **2** and in Figure S4 for **3**), suggesting the involvement of a reactive oxygen species (ROS). The presence of catalase, the scavenger of H_2O_2, had little effect on DNA cleavage (lane 2). In contrast, superoxide dismutase (SOD), the scavenger of $O_2^{-\bullet}$, restricted DNA cleavage markedly (lane 3). When KI (lane 4) and NaN_3 (lane

DOI: 10.1021/acs.inorgchem.6b00028
Inorg. Chem. XXXX, XXX, XXX–XXX

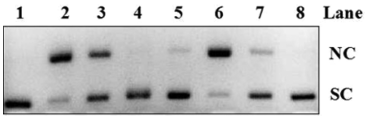

Figure 2. Agarose gel electrophoresis pattern of photocleaved supercoiled pBR322 DNA (31 μM base pair) by **2** (100 μM) upon irradiation (>470 nm) for 30 min in a Tris-CH_3COOH/EDTA buffer (pH 8.0, 8% DMSO). Lanes 1 and 8, DNA alone; lane 2, DNA + **2** + catalase (1000 units/mL); lane 3, DNA + **2** + SOD (1000 units/mL); lane 4, DNA + **2** + KI (50 mM); lane 5, DNA + **2** + NaN_3 (50 mM); lane 6, DNA + **2**; lane 7, DNA + **2** in a N_2 atmosphere. SC and NC denote supercoiled circular and nicked-circular forms, respectively.

5), the well-known scavengers of $^{\bullet}OH$ and $^1O_2$, were present, DNA cleavage was totally inhibited. These results indicate that $^{\bullet}OH$ and $^1O_2$ may be the main ROS responsible for the DNA photocleavage by **2** and **3**. Contrary to **2** and **3**, the DNA photocleavage activity of $[Ru(bpy)_3]^{2+}$ stems from a single $^1O_2$ mechanism.[18]

Because DMSO is a typical scavenger of $^{\bullet}OH$, DNA photocleavage experiments were further carried out in a CH_3COOH/EDTA buffer (pH 8.0) containing 8% CH_3CN (Figure 3 and Figure S5). As expected, efficient cleavage in buffer/CH_3CN was also observed at concentrations lower than those in buffer/DMSO.

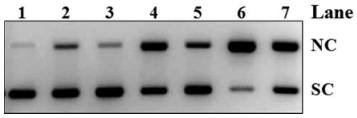

Figure 3. Agarose gel electrophoresis pattern of photocleaved supercoiled pBR322 DNA (31 μM base pair) by **2** upon irradiation (470 nm, 0.32 mW/cm^2) for 40 min in an air-saturated Tris-CH_3COOH/EDTA buffer (pH 8.0, 8% DMSO or 8% CH_3CN). Lane 1, DNA alone; lane 2, DNA + 10 μM **2** + CH_3CN; lane 3, DNA + 10 μM **2** + DMSO; lane 4, DNA + 25 μM **2** + CH_3CN; lane 5, DNA + 25 μM **2** + DMSO; lane 6, DNA + 50 μM **2** + CH_3CN; lane 7, DNA + 50 μM **2** + DMSO. SC and NC denote supercoiled circular and nicked-circular forms, respectively.

We also compared CT-DNA affinities of **1**−**4** using an EB displacement assay (Figures S6−S9), which may play an important role in ROS-mediated DNA photocleavage. As shown in Table 1, the apparent binding constants of **1**−**4** fall in the range 1.72−1.98 × 10^6 M^{-1}. The similar binding constants and the binding order of **1** > **3** > **2** > **4** demonstrate that DNA affinity is not the factor responsible for the poor DNA photocleavage abilities of **1** and **4**.

ROS Generation. We then used the EPR spin-trapping technique to evaluate the $^1O_2$-generation abilities of **1**−**4**. Upon irradiation (>470 nm) of air-saturated CH_3CN solutions of **1**−**4** (1 mM) and 2,2,6,6-tetramethylpiperidine (TEMP, 50 mM), a three-line signal with equal intensities was observed (Figure 4a) with a hyperfine splitting constant of 15.9 G and a *g* factor of 2.0056, in good agreement with TEMPO (the adduct of TEMP and $^1O_2$).[19] Control experiments indicate that O_2, light, and the complexes are all necessary factors. NaN_3 can quench the signal efficiently (Figure S10), further vindicating the $^1O_2$ origin of the signal. We also compared the $^1O_2$-generation abilities of **2** and $[Ru(bpy)_3]^{2+}$ under laser irradiation at 355 nm in air-saturated CH_3CN, where the absorbance of the irradiated samples was adjusted to be the same. As shown in Figure 4b,

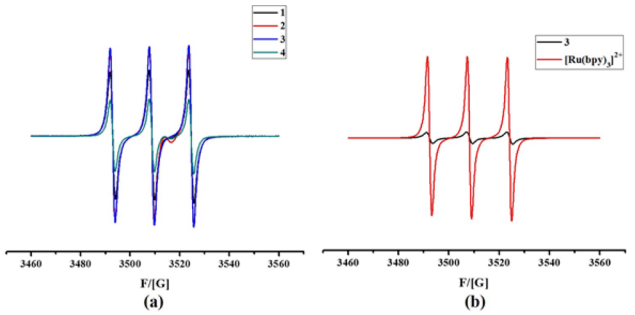

Figure 4. EPR signals obtained (a) upon irradiation (>470 nm) for 2 min of air-saturated CH_3CN solutions of 50 mM TEMP and 1 mM Ru complexes and (b) upon laser irradiation (355 nm) for 2 min of air-saturated CH_3CN solutions of 50 mM TEMP and **2** or $[Ru(bpy)_3]^{2+}$, where the absorbance at 355 nm of the irradiated samples was adjusted to be the same.

$[Ru(bpy)_3]^{2+}$ has an efficiency about 14-fold higher than that of **2** in $^1O_2$ generation. However, $[Ru(bpy)_3]^{2+}$ photocleaved DNA less efficiently than **2** (Figure 1), revealing that $^1O_2$ is not the major ROS accounting for the DNA photocleavage of **2** and **3**.

In the same way, the $^{\bullet}OH$-generation abilities of **1**−**4** were compared using 5,5-dimethyl-1-pyrroline-*N*-oxide (DMPO) as a spin-trapping agent. Upon irradiation (>470 nm) of air-saturated PBS/CH_3CN solutions of **2** and **3** (1 mM) and DMPO (50 mM), a four-line signal with an intensity ratio of 1/2/2/1 was observed (Figure 5 and Figure S11), which exhibits a

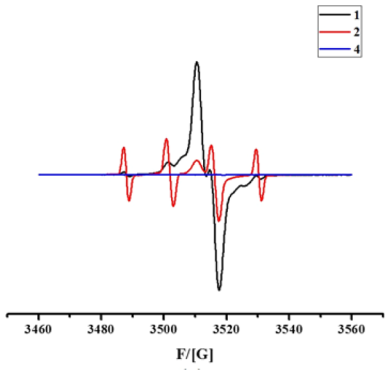

Figure 5. EPR signals obtained upon irradiation (>470 nm) of an air-saturated PBS/CH_3CN (1/1) mixture of 50 mM DMPO and 1 mM examined Ru complexes.

hyperfine splitting constant of $a_H = a_N$ = 14.9 G and a *g* factor of 2.0056, in good agreement with the DMPO/$^{\bullet}OH$ adduct.[19] O_2, light, and the complexes are all necessary for this signal. KI can quench the signal effectively (Figure S11), confirming its $^{\bullet}OH$ origin. Under the same conditions, **1** and **4** did not show this signal, consistent with their poor DNA photocleavage abilities. A chemical-trapping agent of $^{\bullet}OH$, terephthalic acid (TPA), was also utilized to characterize the $^{\bullet}OH$-generation abilities of **1**−**4**. The nonemissive TPA can transform to highly fluorescent 2-hydroxyterephthalic acid by reaction with $^{\bullet}OH$ (Scheme S2). Following the fluorescence intensity changes of the irradiated samples (Figure 6 and Figure S12), a $^{\bullet}OH$-generation order of **2** > **3** ≫ **1**, **4** was obtained in accordance with the EPR results. The generation of $^{\bullet}OH$ is most likely by way of an $O_2^{-\bullet}$ pathway (Scheme 1). The first oxidation potentials of **2** and **3** have a cathodic shift 0.7 V higher than

DOI: 10.1021/acs.inorgchem.6b00028
Inorg. Chem. XXXX, XXX, XXX−XXX

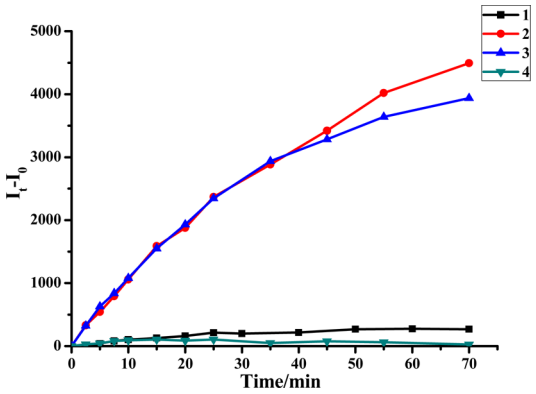

Figure 6. Fluorescence intensity changes at 423 nm as a function of irradiation (470 nm LED, 0.32 mW cm^{-2}) time of aqueous solutions containing 1 mM TPA, 2 mM NaOH, and 100 μM Ru complexes.

that of $[Ru(bpy)_3]^{2+}$ (Table 1), which may dramatically favor the electron transfer from the excited states of **2** and **3** to oxygen. Negligible fluorescence enhancement was observed upon irradiation of the solution of TPA and $[Ru(bpy)_3]^{2+}$ (Figure S13), in line with its single $^1O_2$ mechanism. Interestingly, we found that the presence of NaN_3 may restrict the fluorescence enhancement by **2** and **3** (Figure S14). A possible explanation is that NaN_3 may quench $^{\bullet}OH$,[4b,5a] accounting for its total inhibition of DNA photocleavage of **2** and **3** (Figure 2, lane 5).

Self-Consumption of $^{\bullet}OH$ by 1−4. Because of their less-positive oxidation potentials (Table 1), **1** and **4** should be more efficient in electron donation than **2** and **3**. However, instead of a DMPO/$^{\bullet}OH$ signal, a strong EPR signal with g = 2.003 was obtained in the case of **1** (Figure 5 and Figure S11). This signal was also found in the cases of **2** and **3** but with a much weaker intensity. This signal still occurred in the absence of DMPO (Figure S15) but disappeared in a N_2 atmosphere (Figure S16). The addition of KI can also quench this signal (Figure S11). This signal cannot be assigned to the electron spin located on the Ru fragment, which is generally EPR silent at room temperature in fluid solutions and shows a rhombic g-anisotropy at low temperatures.[9a,14a] On the basis of these facts, we tentatively ascribed this signal to an R-OQN-based radical generated by the attack of $^{\bullet}OH$. Such a process may be more favorable for **1**, leading to its poor apparent $^{\bullet}OH$ generation as well as its low activity in DNA photocleavage. In the cases of **2** and **3**, a halogen atom probably occupies the site of OQN that is more readily attacked by $^{\bullet}OH$, making $^{\bullet}OH$ available to either DMPO or DNA, thus resulting in a higher apparent DMPO/$^{\bullet}OH$ EPR signal and more efficient DNA photocleavage.

Albini and co-workers reported that $^{\bullet}OH$ radicals preferentially attack the 5 and 8 positions of quinoline, and quinoline-5,8-dione may be generated through a series of reactions of the initially formed adduct with $^{\bullet}OH$ and O_2.[20] Similar reactions may occur at the 5 and 6 or 6 and 7 positions of the OQN ligand in the case of **1**, leading to the formation of an M + 2O − 2H product. This is indeed what we observed in the ESI-MS spectra of **1**. After irradiation for 50 min (>470 nm), the strongest m/z signal can be assigned to $[M - PF_6 + 2O - 2H]^+$, as shown in Figure S17. In the cases of **2** and **3**, not only the $[M - PF_6 + 2O - 2H]^+$ signal but also the $[M - PF_6 + 2O - H - X]^+$ signal was observed (Figures S18 and S19). However, the m/z signals of **2** and **3** were still dominated by $[M - PF_6]^+$ upon irradiation for 50 min, in line with our assumption that the 5 position of OQN is the most active site for electrophilic attack of $^{\bullet}OH$ and is protected by an electron-withdrawing halogen atom to some extent. For **4**, irradiation for 50 min led to a total disappearance of the $[M - PF_6]^+$ signal, and the $[M - PF_6 + 2O + 2H]^+$ signal became dominant (Figure S20). The rapid decay rate of **4**, in combination with its different product pattern, may account for its silent EPR behavior and lack of DNA photocleavage capability.

3. CONCLUSIONS

In summary, we demonstrate herein that the OQN-based Ru(II) complexes may generate $^{\bullet}OH$ and cleave DNA efficiently upon visible light irradiation and that halogen substitution on the OQN ligand is crucial for obtaining these properties. With the consideration that the non-innocent ligand-based Ru(II) complexes usually exhibit a long wavelength absorption property, they show promising application potentials as a novel type of PDT agent.

4. EXPERIMENTAL SECTION

Spectroscopic Measurements. ^1H NMR spectra were recorded on a Bruker DMX-400 MHz spectrophotometer using $SiMe_4$ as the standard. High-resolution ESI-MS (HR ESI-MS) spectra were determined on a Bruker APEX IV (7.0T) FT_MS mass spectrometer. UV−visible absorption spectra were taken on a Shimadzu UV-1601PC spectrophotometer. The electrochemical properties were measured on an EG&G model 283 potentiostat/galvanostat in a three-electrode cell with a glassy carbon working electrode, a Pt counter electrode, and a saturated calomel electrode (SCE) as a reference. Cyclic voltammetry was conducted at a scan rate of 50 mV s^{-1} in a N_2-saturated, anhydrous CH_3CN solution containing 0.1 M Bu_4NPF_6 as the supporting electrolyte. The EPR spectra were obtained on a Bruker ESP-300E spectrometer at 9.75 GHz and an X-band with 100 Hz field modulation using TEMP and DMPO as the spin-trapping agents of $^1O_2$ and $^{\bullet}OH$, respectively. Samples were injected quantitatively into specialized quartz capillaries and then illuminated in the cavity of the EPR spectrometer with an Nd:YAG laser at 355 nm (5−6 ns of pulse width, 10 Hz of repetition frequency, 30 mJ/pulse energy) or an LSB610 100 W Hg lamp equipped with a 470 nm long pass glass filter.

EB Displacement Assay. A CT-DNA solution was obtained by dispersing the desired amount of CT-DNA in a PBS (5 mM, pH 7.4) buffer solution and stirring overnight at a temperature below 4 °C. The concentration of CT-DNA was calculated using the extinction coefficient at 260 nm (ε = 6600 M^{-1} cm^{-1}).

The apparent DNA binding constants (K_{app}) of the complexes were determined by monitoring the fluorescence emission changes of mixed solutions of EB (5 μM) and CT-DNA (10 μM) in a PBS buffer with increasing concentrations of the complexes. K_{app} was calculated based on the equation $K_{EB}[EB] = K_{app}[complex]$, where K_{EB} (1×10^7 M^{-1}) represents the binding constant of EB toward CT-DNA, [EB] is the concentration of EB, and [complex] is the concentration of the complex when EB fluorescence is reduced to half of the initial intensity.[21]

Agarose Gel Electrophoresis Experiments. Supercoiled pBR322 plasmid DNA was used as the target for studying DNA damage abilities of the examined complexes. Fifty microliters of supercoiled pBR322 DNA (31 μM base pair) in a Tris-acetic acid-EDTA buffer (pH 8.0) was incubated with **1**−**4**. After irradiation, 20 μL of loading buffer was added. Ten microliters of each sample was taken for agarose gel electrophoresis (in Tris-acetic acid-EDTA buffer, pH 8.0) at 80 V for 1.5 h. The gel was stained with EB (1 mg/L in H_2O) for 0.5 h and then analyzed using a Gel Doc XR system (Bio-Rad). The light sources used in the DNA agarose gel electrophoresis experiments were an LED light (470 nm, 0.32 mW/cm^2) and a 1000 W solar simulator (Oriel 91192) equipped with a 400 or 470 nm long pass glass filter to cut off the short wavelength light.

DOI: 10.1021/acs.inorgchem.6b00028
Inorg. Chem. XXXX, XXX, XXX−XXX

TPA Trapping •OH Experiments. Two milliliter aqueous solutions containing 2 mM NaOH, 1 mM TPA, and 100 μM examined complexes were illuminated at 470 nm (LED light source, 0.32 mW/cm^2) in cuvettes. The fluorescence emission spectral changes of the irradiated solutions were monitored under the excitation wavelength of 315 nm.[22]

■ ASSOCIATED CONTENT

Supporting Information

The Supporting Information is available free of charge on the ACS Publications website at DOI: 10.1021/acs.inorgchem.6b00028.

Materials, synthesis, ESI-MS spectra, UV−vis absorption spectra and cyclic voltammograms of **1**−**4**, DNA gel electrophoresis, EB displacement assay, and EPR spin-trapping and TPA trapping experiments (PDF)

■ AUTHOR INFORMATION

Corresponding Authors

*E-mail: xswang@mail.ipc.ac.cn.
*E-mail: zhouqianxiong@mail.ipc.ac.cn.

Notes

The authors declare no competing financial interest.

■ ACKNOWLEDGMENTS

This work was financially supported by the Ministry of Science and Technology (2013CB933801) and NSFC (21390400, 21172228, 21273259, 21571181, and 21301182).

■ REFERENCES

(1) Armitage, B. *Chem. Rev.* **1998**, *98*, 1171−1200.
(2) Detty, M. R.; Gibson, S. L.; Wagner, S. J. *J. Med. Chem.* **2004**, *47*, 3897−3915.
(3) Clarke, M. J. *Coord. Chem. Rev.* **2003**, *236*, 209−233.
(4) (a) Lincoln, R.; Kohler, L.; Monro, S.; Yin, H.; Stephenson, M.; Zong, R.; Chouai, A.; Dorsey, C.; Hennigar, R.; Thummel, R. P.; McFarland, S. A. *J. Am. Chem. Soc.* **2013**, *135*, 17161−17175. (b) Sun, Y.; Joyce, L. E.; Dickson, N. M.; Turro, C. *Chem. Commun.* **2010**, *46*, 2426−2468. (c) Zhou, Q. X.; Lei, W. H.; Chen, J. R.; Li, C.; Hou, Y. J.; Wang, X. S.; Zhang, B. W. *Chem. - Eur. J.* **2010**, *16*, 3157−3165. (d) Zhou, Q. X.; Lei, W. H.; Sun, Y.; Chen, J. R.; Li, C.; Hou, Y. J.; Wang, X. S.; Zhang, B. W. *Inorg. Chem.* **2010**, *49*, 4729−4731. (e) Zhou, Q. X.; Yang, F.; Lei, W. H.; Chen, J. R.; Li, C.; Hou, Y. J.; Ai, X. C.; Zhang, J. P.; Wang, X. S.; Zhang, B. W. *J. Phys. Chem. B* **2009**, *113*, 11521−11526. (f) Liu, Y.; Hammitt, R.; Lutterman, D. A.; Joyce, L. E.; Thummel, R. P.; Turro, C. *Inorg. Chem.* **2009**, *48*, 375−385.
(5) (a) Poteet, S. A.; Majewski, M. B.; Breitbach, Z. S.; Griffith, C. A.; Singh, S.; Armstrong, D. W.; Wolf, M. O.; MacDonnell, F. M. *J. Am. Chem. Soc.* **2013**, *135*, 2419−2422. (b) Vanderlinden, W.; Blunt, M.; David, C. C.; Moucheron, C.; Kirsch-De Mesmaeker, A.; De Feyter, S. *J. Am. Chem. Soc.* **2012**, *134*, 10214−10221. (c) Boggio-Pasqua, M.; Vicendo, P.; Oubal, M.; Alary, F.; Heully, J.-L. *Chem. - Eur. J.* **2009**, *15*, 2759−2762. (d) Lecomte, J.-P.; Kirsch-De Mesmaeker, A.; Feeney, M. M.; Kelly, J. M. *Inorg. Chem.* **1995**, *34*, 6481−6491.
(6) (a) Zhou, Q. X.; Lei, W. H.; Li, C.; Hou, Y. J.; Wang, X. S.; Zhang, B. W. *New J. Chem.* **2010**, *34*, 137−140. (b) Holcomb, D. R.; Ropp, P. A.; Theil, E. C.; Thorp, H. H. *Inorg. Chem.* **2010**, *49*, 786−795. (c) Evans, S. E.; Mon, S.; Singh, R.; Ryzhkov, L. R.; Szalai, V. A. *Inorg. Chem.* **2006**, *45*, 3124−3132. (d) Stemp, E. D. A.; Arkin, M. R.; Barton, J. K. *J. Am. Chem. Soc.* **1997**, *119*, 2921−2925.
(7) (a) Monro, S.; Scott, J.; Chouai, A.; Lincoln, R.; Zong, R.; Thummel, R. P.; McFarland, S. A. *Inorg. Chem.* **2010**, *49*, 2889−2900. (b) Fu, P. K.-L.; Bradley, P. M.; van Loyen, D.; Durr, H.; Bossmann, S. H.; Turro, C. *Inorg. Chem.* **2002**, *41*, 3808−3810. (c) Augustyn, K. E.; Stemp, E. D. A.; Barton, J. K. *Inorg. Chem.* **2007**, *46*, 9337−9350.
(8) (a) Wang, J.; Newman, J., Jr.; Higgins, S. L. H.; Brewer, K. M.; Winkel, B. S. J.; Brewer, K. J. *Angew. Chem., Int. Ed.* **2013**, *52*, 1262−1265. (b) Wang, J.; Zigler, D. F.; Hurst, N.; Othee, H.; Winkel, B. S. J.; Brewer, K. J. *J. Inorg. Biochem.* **2012**, *116*, 135−139. (c) Holder, A. A.; Swavey, S.; Brewer, K. J. *Inorg. Chem.* **2004**, *43*, 303−308. (d) Swavey, S.; Brewer, K. J. *Inorg. Chem.* **2002**, *41*, 6196−6198.
(9) (a) Zhao, H. C.; Fu, B.-L.; Schweinfurth, D.; Harney, J. P.; Sarkar, B.; Tsai, M.-K.; Rochford, J. *Eur. J. Inorg. Chem.* **2013**, *25*, 4410−4420. (b) Cazacu, M.; Shova, S.; Soroceanu, A.; Machata, P.; Bucinsky, L.; Breza, M.; Rapta, P.; Telser, J.; Krzystek, J.; Arion, V. B. *Inorg. Chem.* **2015**, *54*, 5691−5706.
(10) (a) Kaim, W. *Inorg. Chem.* **2011**, *50*, 9752−9765. (b) Eisenberg, R. *Coord. Chem. Rev.* **2011**, *255*, 825−836. (c) Kaim, W.; Schwederski, B. *Coord. Chem. Rev.* **2010**, *254*, 1580−1588. (d) Ray, K.; Petrenko, T.; Wieghardt, K.; Neese, F. *Dalton Trans.* **2007**, 1552−1566. (e) Ward, M. D.; McCleverty, J. A. *J. Chem. Soc., Dalton Trans.* **2002**, 275−288.
(11) Boyer, J. L.; Rochford, J.; Tsai, M.-K.; Muckerman, J. T.; Fujita, E. *Coord. Chem. Rev.* **2010**, *254*, 309−330.
(12) (a) Tong, L.; Wang, Y.; Duan, L.; Xu, Y.; Cheng, X.; Fischer, A.; Ahlquist, M. S. G.; Sun, L. *Inorg. Chem.* **2012**, *51*, 3388−3398. (b) Wada, T.; Tsuge, K.; Tanaka, K. *Inorg. Chem.* **2001**, *40*, 329−337. (c) Wada, T.; Tsuge, K.; Tanaka, K. *Angew. Chem., Int. Ed.* **2000**, *39*, 1479−1482.
(13) Zhao, H. C.; Harney, J. P.; Huang, Y.-T.; Yum, J.-H.; Nazeeruddin, Md. K.; Grätzel, M.; Tsai, M.-K.; Rochford, J. *Inorg. Chem.* **2012**, *51*, 1−3.
(14) (a) Bellinger-Buckley, S.; Chang, T.-C.; Bag, S.; Schweinfurth, D.; Zhou, W.; Torok, B.; Sarkar, B.; Tsai, M.-K.; Rochford, J. *Inorg. Chem.* **2014**, *53*, 5556−5567. (b) El Ojaimi, M.; Thummel, R. P. *Inorg. Chem.* **2011**, *50*, 10966−10973. (c) Sears, R. B.; Joyce, L. E.; Turro, C. *Photochem. Photobiol.* **2010**, *86*, 1230−1236. (d) Warren, J. T.; Chen, W.; Johnston, D. H.; Turro, C. *Inorg. Chem.* **1999**, *38*, 6187−6192. (e) Bhattacharya, S. *Polyhedron* **1993**, *12*, 235−239. (f) Dragonetti, C.; Valore, A.; Colombo, A.; Magni, M.; Mussini, P.; Roberto, D.; Ugo, R.; Valsecchi, A.; Trifiletti, V.; Manfredi, N.; Abbotto, A. *Inorg. Chim. Acta* **2013**, *405*, 98−104. (g) Leung, C.-F.; Wong, C.-Y.; Ko, C.-C.; Yuen, M.-C.; Wong, W.-T.; Wong, W.-Y.; Lau, T.-C. *Inorg. Chim. Acta* **2009**, *362*, 1149−1157.
(15) (a) Heidary, D. K.; Howerton, B. S.; Glazer, E. C. *J. Med. Chem.* **2014**, *57*, 8936−8946. (b) Yang, L. C.; Zhang, J. N.; Wang, C.; Qin, X. Y.; Yu, Q. Q.; Zhou, Y. H.; Liu, J. *Metallomics* **2014**, *6*, 518−531. (c) Gobec, M.; Kljun, J.; Sosič, I.; Mlinarič-Raščan, I.; Uršič, M.; Gobec, S.; Turel, I. *Dalton Trans.* **2014**, *43*, 9045−9051. (d) Kubanik, M.; Holtkamp, H.; Söhnel, T.; Jamieson, S. M. F.; Hartinger, C. G. *Organometallics* **2015**, *34*, 5658−5668.
(16) (a) Hirakawa, T.; Nosaka, Y. *Langmuir* **2002**, *18*, 3247−3254. (b) Al-Ekabi, H.; Serpone, N. *J. Phys. Chem.* **1988**, *92*, 5726−5731. (c) Izumi, I.; Fan, F.-R. F.; Bard, A. J. *J. Phys. Chem.* **1981**, *85*, 218−223.
(17) Ngo, K. T.; Lee, N. A.; Pinnace, S. D.; Szalda, D. J.; Weber, R. T.; Rochford, J. *Inorg. Chem.* **2016**, *55*, 2460−2472.
(18) (a) Burrows, C. J.; Muller, J. G. *Chem. Rev.* **1998**, *98*, 1109−1151. (b) Fleisher, M. B.; Waterman, K. C.; Turro, N. J.; Barton, J. K. *Inorg. Chem.* **1986**, *25*, 3549−3551. (c) Chattopadhyay, S. K.; Kumar, C. V.; Das, P. K. *J. Photochem.* **1984**, *24*, 1−9.
(19) Xu, S. J.; Zhang, X. X.; Chen, S.; Zhang, M. H.; Shen, T. *Photochem. Photobiol. Sci.* **2003**, *2*, 871−876.
(20) Cermenati, L.; Pichat, P.; Guillard, C.; Albini, A. *J. Phys. Chem. B* **1997**, *101*, 2650−2658.
(21) Lee, M.; Rhodes, A. L.; Wyatt, M. D.; Forrow, S.; Hartley, J. A. *Biochemistry* **1993**, *32*, 4237−4245.
(22) Fang, C.; Jia, H.; Chang, S.; Ruan, Q. F.; Wang, P.; Chen, T.; Wang, J. F. *Energy Environ. Sci.* **2014**, *7*, 3431−3438.

DOI: 10.1021/acs.inorgchem.6b00028
Inorg. Chem. XXXX, XXX, XXX−XXX